Acta Biochim Biophys Sin 2023, 55(4): 649–660
https://doi.org/10.3724/abbs.2023010
Advance Access Publication Date: 14 February 2023
Original Article

Original Article

lncRNA *ELFN1-AS1* promotes proliferation, migration and invasion and suppresses apoptosis in colorectal cancer cells by enhancing *G6PD* activity

Fahong Wu, Wei Zhang, Hangzhi Wei, Hanwei Ma, Guangxian Leng, and Youcheng Zhang*

Department of General Surgery, Hepatic-biliary-pancreatic Institute, Lanzhou University Second Hospital, Lanzhou 730030, China
*Correspondence address. Tel: +86-13919975286; E-mail: zhangyouchengphd@163.com

Received 22 July 2022 Accepted 23 November 2022

Abstract

Tumour cells change their metabolic patterns to support high proliferation rates and cope with oxidative stress. The lncRNA *ELFN1-AS1* is highly expressed in a wide range of cancers and is essential to the proliferation and apoptosis of tumour cells. Nevertheless, its function in the metabolic reprogramming of tumour cells is unclear. Here we show that *ELFN1-AS1* promotes glucose consumption as well as lactate and NADPH production. Database searching, bioinformatics analysis, RNA immunoprecipitation (RIP) and RNA pull-down assays show that *ELFN1-AS1* enhances glucose-6-phosphate dehydrogenase (*G6PD*) expression and activates the pentose phosphate pathway (PPP) by promoting *TP53* degradation. In addition, luciferase reporter assay and chromatin immunoprecipitation (ChIP) show that *YY1* binds to the *ELFN1-AS1* promoter to promote transcriptional activation of *ELFN1-AS1*. Consistent with the *in vitro* experiments, knockdown of *ELFN1-AS1* impedes the growth of tumours transplanted into mice by inhibiting the expression of *G6PD*. In conclusion, this study reveals that *ELFN1-AS1* activates the PPP, and validates the regulatory role of the *YY1*/*ELFN1-AS1*/*TP53*/*G6PD* axis in colorectal cancer.

Key words lncRNA *ELFN1-AS1*, colorectal cancer, YY1, TP53, G6PD

Introduction

Carcinogenesis depends on the reprogramming of tumour cell metabolism as a natural consequence of oncogenic mutations [1]. As first observed by Otto Warburg, tumour cells tend to use large amounts of glucose through aerobic glycolysis [2]. This metabolic change can not only support the energy and macromolecule requirements of tumour cells but also lead to the formation of a microenvironment conducive to tumour cell growth and survival [3]. Over the past century, key studies on tumour metabolism have identified metabolic reprogramming as a major contributor to tumour progression and have also detected alterations in metabolic reprogramming far exceeding initial expectations [4]. Activation of the pentose phosphate pathway (PPP) is an important consequence of metabolic reprogramming [5]. The PPP is a branch of glycolysis that is catalysed by hexokinase and consumes glucose-6-phosphate as the main substrate. The PPP can produce nicotinamide adenine dinucleotide phosphate (NADPH), which is necessary for the production of reduced glutathione, and glutathione can scavenge reactive oxygen species (ROS) to maintain cell homeostasis. The PPP also generates ribulose-5-phosphate (Ru5P) for nucleotide biosynthesis [6]. Although the PPP plays a key role in tumorigenesis, its specific regulatory mechanism remains unclear.

Long noncoding RNAs (lncRNAs) are RNA molecules with transcript lengths of over 200 nt that have no protein-coding potential [7–9]. lncRNAs in the nucleus are mainly involved in epigenetic and transcriptional gene regulation processes, including histone modification, DNA methylation regulation, chromatin remodelling, chromatin modification complex formation, transcription factor activity, and nuclear protein expression [10–15]. Moreover, lncRNAs in the cytoplasm are mainly involved in gene regulation at the posttranscriptional and translational levels; for example, they interact with proteins in the cytoplasm to regulate mRNA metabolism [16–18]. Above results indicate that lncRNAs are extensively involved in the proliferation, migration, invasion and apoptosis of cancer cells.

The lncRNA *ELFN1-AS1* is located in the intron of the *ELFN1* gene

on chromosome 7. Computer simulation analysis and experimental detection of *ELFN1-AS1* transcripts in tumours of different histological origins have revealed that this lncRNA is predominantly expressed in human tumours [19]. Further studies revealed that *ELFN1-AS1* is expressed in both the cytoplasm and nucleus [20]. In recent years, researchers have found that *ELFN1-AS1* regulates the progression of cancer. Zhang *et al.* [21] found that knockdown of *ELFN1-AS1* can upregulate *GFPT1* by inhibiting miR-183-3p, thereby inhibiting tumour cell migration, invasion and proliferation in oesophageal cancer. Jie *et al.* [22] found that in ovarian cancer, *ELFN1-AS1* promotes tumour cell development by directly regulating *CLDN4* expression via miR-497-3P. A recent study reported that *ELFN1-AS1* is highly expressed in colorectal cancer (CRC) and enhances the proliferation, migration and anti-apoptotic functions of CRC cells through the miR-4644/TRIM44 axis [23]. However, whether *ELFN1-AS1* is engaged in modulating the metabolic reprogramming of tumour cells has not been investigated thus far.

In this study, we found that *ELFN1-AS1* activates the PPP and validated the regulatory role of the *YY1/ELFN1-AS1/TP53/G6PD* axis in CRC, which offers a new theory for CRC treatment.

Materials and Methods

Patients and specimens

Forty CRC tissues and matched normal tissues were obtained from the Lanzhou University Second Hospital (Lanzhou, China). In addition, the clinicopathological features of these forty CRC patients were collected for clinicopathological exploration of *ELFN1-AS1*. None of the patients were treated with radiotherapy or chemotherapy prior to surgery, and all CRC diagnoses were confirmed by the pathology department. Informed consents were obtained from all patients before specimen collection. In addition, the investigation was authorized by the Ethics Committee of the Academic Medical Center of the Lanzhou University Second Hospital (No. 2021A-488). The study was performed in accordance with the Declaration of Helsinki.

Online databases

Totally, 568 CRC samples and 44 normal samples were obtained from The Cancer Genome Atlas (TCGA) (https://www.ncbi.nlm.nih.gov/geo/), and 566 CRC samples and 19 normal samples were obtained from Gene Expression Omnibus (GEO) (https://www.ncbi.nlm.nih.gov/geo/). Gene Set Enrichment Analysis (GSEA) enrichment analysis was used to predict the signaling pathways associated with *ELFN1-AS1* (http://software.broadinstitute.org/gsea/). RNA Interactome and string was used to predict the transcription factors that bind to *ELFN1-AS1* (http://www.rnainter.org/). catRAPID was used to predict the binding potential of *ELFN1-AS1* to *TP53* (http://s.tartaglialab.com/page/catrapid_group). PROMO databases (http://alggen.lsi.upc.es/cgibin/promo_v3/promo/promoinit.cgi?dirDB=TF_8.3) and GeneCar-ds (https://www.genecards.org/) were used to predict transcription factors that bind to the *ELFN1-AS1* promoter.

Cell culture and transfection

SW480, RKO and HCT116 human CRC cells were obtained from the Cell Bank of the Type Culture Collection of the Chinese Academy of Sciences (Shanghai, China). All the above CRC cells were cultured in DMEM containing 12% fetal bovine serum (Gibco, Grand Island, USA) at 37°C under 5% CO_2. Short hairpin RNAs targeting *ELFN1-AS1* or *TP53* (shELFN1-AS1#1, shELFN1-AS1#2, and shTP53) were purchased from GenePharma (Shanghai, China). The group with simultaneous targeting of *ELFN1-AS1* and *TP53* by short hairpin RNA was denoted as the shELFN1-AS1 + shTP53 group. *G6PD* was overexpressed using a vector containing the full-length sequence of *G6PD* cDNA (GenePharma). Cells with simultaneous knockdown of *ELFN1-AS1* and overexpression of *G6PD* were denoted as the shELFN1-AS1 + G6PD group. Afterwards, RKO and HCT116 cells were transfected using Lipofectamine™ 2000 (Invitrogen, Karlsbad, USA). Stable cell lines were selected with 2 μg/mL puromycin. All of the above interference and overexpression construct sequences are listed in Supplementary Table S1.

Western blot analysis

Western blotting experiments were performed as previously described [24]. The antibodies used in this research were as follows: anti-human β-actin (AF7018; Affinity Biosciences, Cincinnati, USA), anti-human G6PD (ab210702; Abcam, Cambridge, UK), anti-human TP53 (9282; Cell Signaling Technology, Boston, USA), anti-human E-cadherin (ab231303; Abcam), anti-human N-cadherin (ab207608; Abcam), anti-human MMP-9 (AF5228; Affinity Biosciences), anti-human Bcl-2 (AF6139; Affinity Biosciences), anti-human cleaved caspase-3 (AF7022; Affinity Biosciences), anti-human Cyt-C (AF0146; Affinity Biosciences), and anti-human YY1 (ABP60802; Abbkine, Wuhan, China).

qRT-PCR

After the cells were successfully transfected with the target gene, they were lysed with lysis buffer (Servicebio, Wuhan, China) at 4°C for 30 min. The cell concentrations were determined with a NanoDrop 2000 (Thermo Fisher Scientific, Waltham, USA). Total RNA was extracted from cells and tissues using TransZol reagent (Servicebio, Wuhan, China). A Revert Aid First Strand cDNA Synthesis Kit (Servicebio) was used for reverse transcription. First, the polymerase was activated at 95°C for 30 s, followed by denaturation at 95°C for 15 s. Next, annealing was at 55°C–65°C for 10 s, and extension was at 72°C for 30 s. This amplification was run for 40 cycles. The fluorescence during PCR was determined using a CFX96 real-time system (Bio-Rad, Shanghai, China). The $2^{-\Delta\Delta Ct}$ method was used to determine the relative gene expression, and *β-actin* was used as an internal reference gene. The PCR primers are listed in Supplementary Table S2.

Transwell assay

The migration and invasion abilities of CRC cells were evaluated by transwell assay. Each well above the transwell chambers (Servicebio) was inoculated with 5×10^4 cells and serum-free DMEM was added, and 10% fetal bovine serum was added below the chambers. The cells were incubated for 24 h, fixed in 4% paraformaldehyde (Servicebio) and stained with 0.1% crystal violet (Servicebio).

CCK-8 assay and colony formation assay

Where 96-well plates were inoculated with 2.5×10^3 cells/well, 10 μL CCK-8 (Servicebio) was added to each well, incubated at 37°C for 4 h, and OD values were measured using a microplate reader (ThermoFisher Scientific, Waltham, USA) at 24, 48, 72 and 96 h. Colony formation assay was conducted as follows: 1×10^3 cells/well were inoculated in a 6-well plate for two weeks, then fixed in paraformaldehyde and stained with 0.1% crystal violet.

Analyses of glucose consumption, lactate production, G6PD enzyme activity, and intracellular NADPH level

RKO and HCT116 cells were transfected with shRNA expression vectors or overexpression vectors. Glucose level in CRC cells was determined with a Glucose content assay kit. Lactate production was measured with a lactate assay kit. *G6PD* activity was assessed with a *G6PD* assay kit. The assay kits mentioned above were purchased from Cominbio (Suzhou, China). Intracellular NADPH level was assessed with an NADPH content assay kit (Solarbio, Beijing, China). To assess *G6PD* activity in CRC samples, tissues were homogenized, and enzyme activity was assessed with the *G6PD* assay kit and calculated relative to that of the control group. The total protein amount was measured using the ELISA assay kit (Beyotime, Shanghai, China).

Apoptosis assay and intracellular ROS accumulation analysis

RKO and HCT116 cell apoptosis was assessed with a CytoFLEX flow cytometer (Beckman, Brea, USA) using the Annexin V-Alexa Fluor 647/PI Apoptosis Detection Kit (Solarbio). Cells in good growth conditions were grown in culture flasks. The cells were then digested, washed and incubated with PI and Annexin V-Alexa Fluor 647 according to the manufacturer's instructions, and the fluorescence intensities were measured with the CytoFLEX flow cytometer. The RKO and HCT116 cells were collected and incubated with DCFH-DA (Solarbio) for 30 min at 37°C. After incubation, the cells were washed three times with PBS, and the fluorescence was determined with the CytoFLEX flow cytometer.

RNA immunoprecipitation assay

RIP was performed using a RIP kit (BersinBio™, Guangzhou, China). Briefly, RKO and HCT116 cells were lysed, and the lysates were incubated with magnetic beads conjugated with anti-TP53 monoclonal antibodies or control IgG. Then, RNA was eluted from the magnetic beads, and the *ELFN1-AS1* level was measured by qRT-PCR. The RIP assay was repeated three times independently.

RNA pull-down assay

RNA pull-down was determined using an RNA pull-down kit (BersinBio™). A biotin *ELFN1-AS1* probe was used to label the RNA in an *in vitro* transcriptional assay, and the RNA was then incubated with protein extracts to form RNA–protein complexes. The complexes bound to streptavidin-labelled magnetic beads, which separated them from the other components of the incubation solution. After elution of the complexes, specific *ELFN1-AS1*-binding proteins were detected by western blot analysis. The antisense sequence of *ELFN1-AS1* was used as a negative control (NC).

Luciferase reporter assays and chromatin immunoprecipitation (ChIP)

Small interfering RNAs (siRNAs) were designed by GenePharma. These included two siRNAs targeting *YY1* (siYY1#1 sense sequence: 5′-CCUCCUGAUUAUUCAGAAUTT-3′; and siYY1#2 sense sequence: 5′-CUGGCAGAAUUUGCUAGAATT-3′). The pGL3 luciferase reporter vector for the *ELFN1-AS1* promoter was constructed by GenePharma. Then, CRC cells were cotransfected with pGL3-basic (2 μg) and Renilla luciferase (20 ng) for 24 h using Lipofectamine 2000. Luciferase activity was determined with a dual luciferase reporter enzyme assay system (GenePharma). Renilla luciferase activity was normalized. A chromatin immunoprecipitation kit (Thermo Fisher Scientific) was used based on provided instructions. IgG antibody was used as a control. PCR was used to amplify bound DNA, which was then assessed via electrophoretic separation on a 2% agarose gel.

Ubiquitination assay

To further reveal whether ELNF1-AS1 regulates *TP53* stability, the expression of *TP53* protein in RKO and HCT116 cells treated with CHX (MCE, Merced, USA) was detected at 0, 30 and 60 min, respectively. CRC cells were treated with MG132 (MCE) for 5 h. Then, cell lysate and agarose Protein A + G (Thermo Fisher Scientific) were added and sealed in refrigerator at 4°C for 2 h. Primary antibody was added and incubated overnight. Agarose-containing Protein A + G was added and incubated at 4°C for about 5 h to obtain the target protein.

Immunohistochemistry (IHC)

IHC was performed as previously described [25]. Primary antibodies for Ki-67, N-cadherin, E-cadherin, G6PD, Bcl-2, cleaved caspase-3 were incubated with tissue sections overnight at 4°C. The random fields per section were captured at the same exposure value under an optical microscope (Olympus, Tokyo, Japan). The result was evaluated by the following methods: mean optical density (MOD) = integral optical density (IOD)/positive area.

In vivo assays

All animal experiments were approved by the Experimental Animal Welfare Ethics Committee of the Lanzhou University Second Hospital (No. D2021-259). Male BALB/c nude mice (5 weeks old) were purchased from Jiangsu GemPharmatech (Nanjing, China). Male BALB/c nude mice were kept in the SPF facility of the Animal Center of Lanzhou University (Lanzhou, China), and their care was in accordance with institutional guidelines. HCT116 cells were stably transfected with the NC, shELFN1-AS1 and shELFN1-AS1 + G6PD groups constructs. HCT116 cells (5×10^6) were suspended in 100 μL of Matrigel and subcutaneously injected into the axillae of nude mice. After the mice formed tumours, tumour volume was measured every 3 days. Finally, the mice were sacrificed, and the tumours were excised and weighed.

Statistical analysis

SPSS 23.0 software was used for statistical analysis. Student's *t*-test (two-tailed), chi-square *t* test, and one-way ANOVA were used for data analysis. Data were presented as the mean ± SD of three independent trials, and differences were regarded as statistically significant when $P < 0.05$.

Results

ELFN1-AS1 regulates glucose metabolism in tumour cells

First, we found that the expression of *ELFN1-AS1* in CRC cells was higher than that in normal colorectal FHC cells (Figure 1A). We constructed *ELFN1-AS1*-knockdown strains and selected two sequences with the most significant *ELFN1-AS1* knockdown for further study (Figure 1B). As shown in Figure 1C–E, knockdown of *ELFN1-AS1* suppressed the proliferation, migration and invasion of the cells. Then, we found that *ELFN1-AS1* promoted the PPP by GSEA (Figure 1F). We further investigated glucose metabolism and found that knockdown of *ELFN1-AS1* significantly downregulated

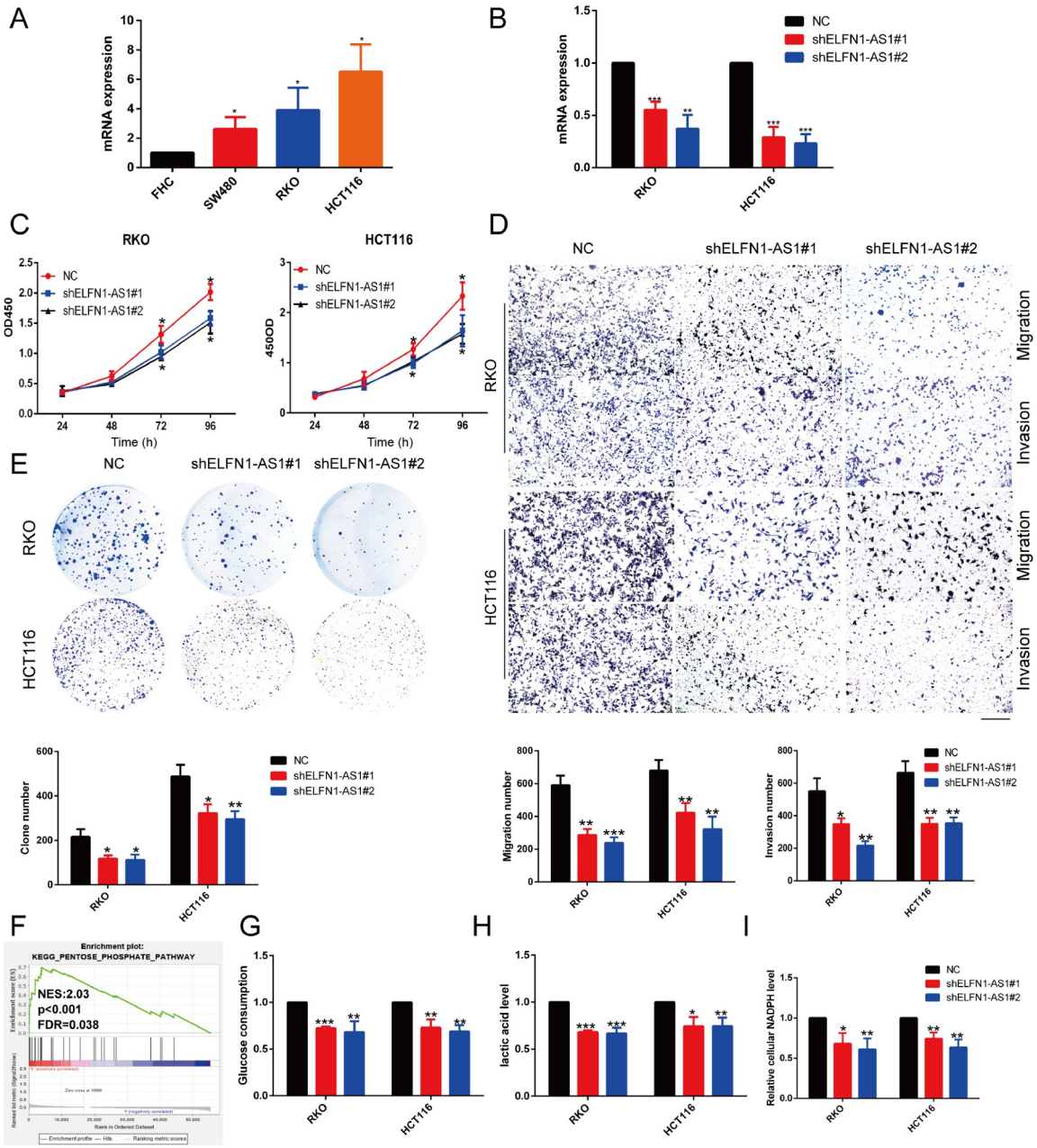

Figure 1. *ELFN1-AS1* regulates glucose metabolism in tumour cells (A) The expression of *ELFN1-AS1* in CRC cells was higher than that in normal colorectal FHC cells. (B) qRT-PCR was used to validate the knockout efficiency of *ELFN1-AS1*. (C) A CCK-8 assay was used to evaluate the proliferation of CRC cells. (D) Transwell assays were used to assess the ability of transfected cells to migrate and invade. The histogram shows the numbers of migrating and invading cells (scale bar = 200 μm). (E) A colony formation experiment was conducted on CRC cell lines that were successfully transfected. The histogram shows the number of cell colonies formed. (F) The GSEA results showed that *ELFN1-AS1* was related to the PPP. The horizontal axis represents each downstream gene, and the vertical axis represents the enrichment score (ES). NES, normalized enrichment score. FDR, false discovery rate (represents the *P* value corrected by multiple hypothesis testing). (G–I) Glucose consumption, lactic acid and NADPH production levels in CRC cells transfected with the NC construct or shELFN1-AS1. Data are shown as the mean ± SD. $^{*}P < 0.05$, $^{**}P < 0.01$, $^{***}P < 0.001$.

glucose consumption, lactate and NADPH production (Figure 1G–I). These data suggested that *ELFN1-AS1* promoted glucose metabolism in CRC cells.

G6PD is an important target for *ELFN1-AS1* in promoting CRC progression

To further investigate the mechanism of PPP activation by *ELFN1-AS1*, we chose *G6PD*, which is the first rate-limiting enzyme of the PPP, as the study subject. Overexpression of *G6PD* promoted the proliferation, migration and invasion of tumour cells (Supplementary Figure S1). We knocked down *ELFN1-AS1* and found that *G6PD* protein expression and activity were significantly inhibited in cells (Figure 2A,B). However, both the protein expression and activity of *G6PD* were restored by *G6PD*

overexpression (Figure 2C,D). Next, we found that downregulation of *ELFN1-AS1* expression significantly suppressed the proliferation, migration and invasion of tumour cells, while overexpression of *G6PD* attenuated this inhibitory effect (Figure 2E–G). We further found that downregulation of *ELFN1-AS1* expression in CRC cells enhanced the expression of *E-cadherin* and suppressed the expressions of *N-cadherin* and *MMP-9*; however, overexpression of *G6PD* blocked these effects (Figure 2H).

NADPH is an important product of the PPP and a key factor in the inhibition of cellular ROS accumulation. We found that downregulation of *ELFN1-AS1* expression significantly inhibited intracellular NADPH production, while overexpression of *G6PD* attenuated this inhibitory effect (Figure 3A). Flow cytometric analysis revealed that downregulation of *ELFN1-AS1* expression significantly promoted ROS accumulation and apoptosis in CRC cells, but both of these effects were reversed by overexpression of *G6PD* (Figure 3B,C). We found that downregulation of *ELFN1-AS1* in CRC cells inhibited the expression of *Bcl-2* and promoted the expressions of *cleaved caspase-3* and *Cyt-C*. Further studies revealed that overexpression of *G6PD* attenuated this effect (Figure 3D). These data indicated that *ELFN1-AS1* significantly inhibited ROS accumulation and apoptosis by *G6PD* in CRC cells.

ELFN1-AS1 regulates *G6PD* expression and activity by *TP53* degradation

We applied RNAInter to predict 320 molecules that interact with *ELFN1-AS1* (Supplementary Table S3) and further analysed these 320 molecules using the Search Tool for the Retrieval of Interacting Genes/Proteins database. Since the combined score of *TP53* was the highest, we speculated that *ELFN1-AS1* may regulate *G6PD* expression via *TP53* (Supplementary Table S4). We found that knockdown of *TP53* promoted the protein expression and activity of *G6PD* (Figure 4A,B). Next, we used another algorithm based on catRAPID fragments and the propensity of peptide and nucleotide sequence fragments to interact individually and further revealed that *ELFN1-AS1* may bind to the *TP53* protein (Figure 4C). The specific binding sites are shown in Supplementary Table S5, and the results verified the interaction between *ELFN1-AS1* and *TP53* (Figure 4D,E). Knockdown of *ELFN1-AS1* reduced *G6PD* expression and activity, while further knockdown of *TP53* attenuated this inhibition (Figure 4F,G).

Next, we investigated whether *ELFN1-AS1* could regulate *TP53* mRNA expression. We found that knockdown of *ELFN1-AS1* had no significant effect on *TP53* mRNA expression (Figure 4H). Immunoprecipitation assay showed that there was an interaction between *MDM2* and *TP53* (Supplementary Figure S2A). We detected the expression of *TP53* protein in RKO and HCT116 cells treated with CHX, and found that shELFN1-AS1 increased the stability of *TP53* protein (Figure 4I and Supplementary Figure S2B). In addition, the proteasome inhibitor MG132 eliminated the regulation of *TP53* expression by the downregulation of *ELFN1-AS1* (Figure 4J and Supplementary Figure S2C). We further found that knockdown of *ELFN1-AS1* reduced the ubiquitination of *TP53*, while overexpression of *MDM2* attenuated this inhibition (Figure 4K,L and Supplementary Figure S2D,E). These data indicated that *ELFN1-AS1* enhanced *G6PD* expression and activated the PPP by promoting *TP53* degradation.

YY1 promotes *ELFN1-AS1* transcription in CRC cells

To determine the upstream regulatory mechanism of *ELFN1-AS1* in CRC cells, we used PROMO and GeneCards to predict 19 and 105 transcription factors (Supplementary Table S6), respectively, that may bind to the promoter of *ELFN1-AS1*. *YY1* was obtained after observing the intersection of both databases (Figure 5A). Then, we knocked down *YY1* in CRC cells (Figure 5B). We found that knockdown of *YY1* suppressed the transcription of *ELFN1-AS1* and the expression of *G6PD* (Figure 5C,D). To further assess whether *YY1* could bind to the promoter of *ELFN1-AS1* to promote transcription of *ELFN1-AS1*, we verified the interaction between the promoter sequence and *YY1* by ChIP and fluorescence dual reporter assays (Figure 5E–G). These data indicated that *YY1* bound to the *ELFN1-AS1* promoter to promote transcriptional activation of *ELFN1-AS1*.

The *ELFN1-AS1*/*G6PD* axis alters tumour growth

To further verify the effect of the *ELFN1-AS1*/*G6PD* axis *in vivo*, we used an xenograft nude mouse model with subcutaneous injection of HCT116 cells from the NC, shELFN1-AS1 and shELFN1-AS1 + G6PD groups. Twenty-five days later, the mice were euthanized, and tumours were collected (Figure 6A). The results revealed that downregulation of *ELFN1-AS1* expression inhibited tumour growth, while overexpression of *G6PD* attenuated this inhibitory effect (Figure 6B,C). The body weights of the nude mice were not significantly different among the three groups (Figure 6D). As shown in Figure 6E, downregulation of *ELFN1-AS1* expression significantly reduced the tumour weight in nude mice, while overexpression of *G6PD* restored the tumour weight (Figure 6E). IHC results revealed that compared with that in the control group, *Ki-67*, *N-cadherin*, *G6PD* and *Bcl-2* expressions in tumour tissues were downregulated in the shELFN1-AS1 group, while *E-cadherin* and *cleaved caspase-3* expressions were upregulated. Further studies revealed that overexpression of *G6PD* attenuated this effect (Figure 6F,G). In addition, the results of *G6PD* protein and activity were consistent with the IHC images (Figure 6H–J). These data indicated that *ELFN1-AS1* significantly promoted the tumour growth via *G6PD*.

Correlations of *ELFN1-AS1*/*G6PD* co-expression with clinicopathological characteristics

The results of TCGA and GSE39582 databases showed that *ELFN1-AS1* was highly expressed in CRC (Figure 7A,B). Next, we detected the expression of *ELFN1-AS1* in CRC and matched normal tissues. The results confirmed that the overall level of *ELFN1-AS1* expression was higher in CRC than in normal tissues (Figure 7C). As shown in Figure 7D, *ELFN1-AS1* expression was also higher in CRC than in matched normal tissues (Figure 7D). Western blot analysis showed that *G6PD* expression was high in CRC, which was consistent with *ELFN1-AS1* expression (Figure 7E). These data revealed that *YY1* mRNA and *G6PD* protein expressions were positively related to *ELFN1-AS1* expression (Figure 7F,G). Further study found that the *ELFN1-AS1*/*G6PD* co-expression was related to lymph node metastasis and TNM stage (Supplementary Table S7). These data indicated that *ELFN1-AS1* and *G6PD* expression may be critical in the tumorigenesis and progression of CRC patients.

Discussion

CRC is the fifth leading cause of cancer-related deaths in China, and the incidence rate continues to rise each year. Unfortunately, the

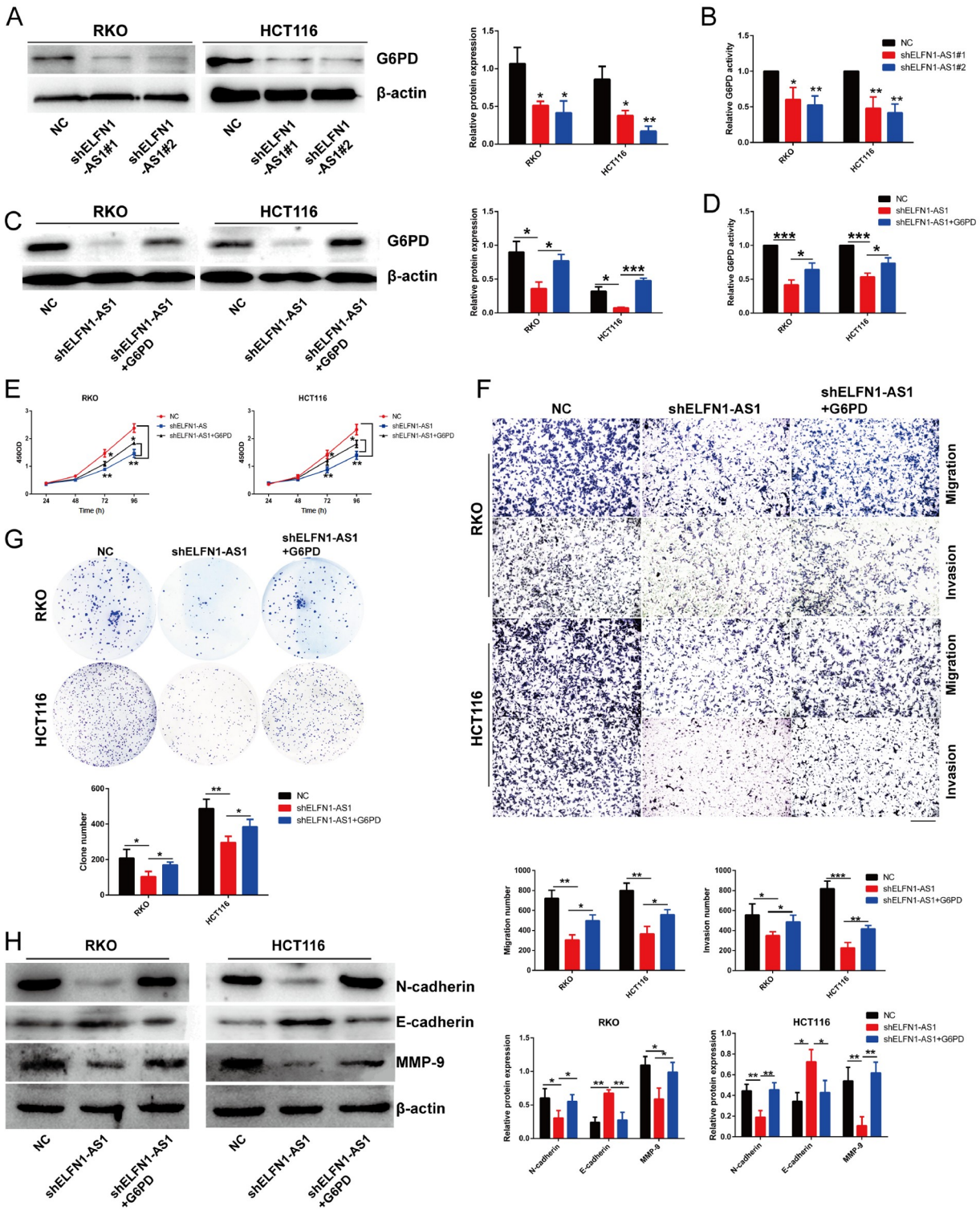

Figure 2. *G6PD* is an important target for *ELFN1-AS1* (A) Western blot analysis was used to analyse the expression of *G6PD* in CRC cells transfected with the NC construct or shELFN1-AS1. (B) *G6PD* activity in the NC and shELFN1-AS1 groups. (C) Expression levels of *G6PD* protein in CRC cells with NC transfection, shELFN1-AS1 transfection or shELFN1-AS1 + G6PD transfection (*ELFN1-AS1* knockout together with *G6PD* overexpression). (D) *G6PD* activity in CRC cells transfected with the NC construct, shELFN1-AS1 or shELFN1-AS1 + G6PD. (E) A CCK-8 assay was used to evaluate proliferation in the different groups. (F) Transwell assays were used to detect the ability of transfected cells to migrate and invade. The histogram shows the numbers of migrating and invading cells (scale bar = 200 μm). (G) A 14-day colony formation experiment was conducted for the different groups. The histogram shows the number of cell colonies that formed. (H) Knockdown of *ELFN1-AS1* in CRC cells enhanced the expression of *E-cadherin* and suppressed the expressions of *N-cadherin* and *MMP-9*, while overexpression of *G6PD* blocked these effects. Data are shown as the mean ± SD. $^{*}P < 0.05$, $^{**}P < 0.01$, $^{***}P < 0.001$.

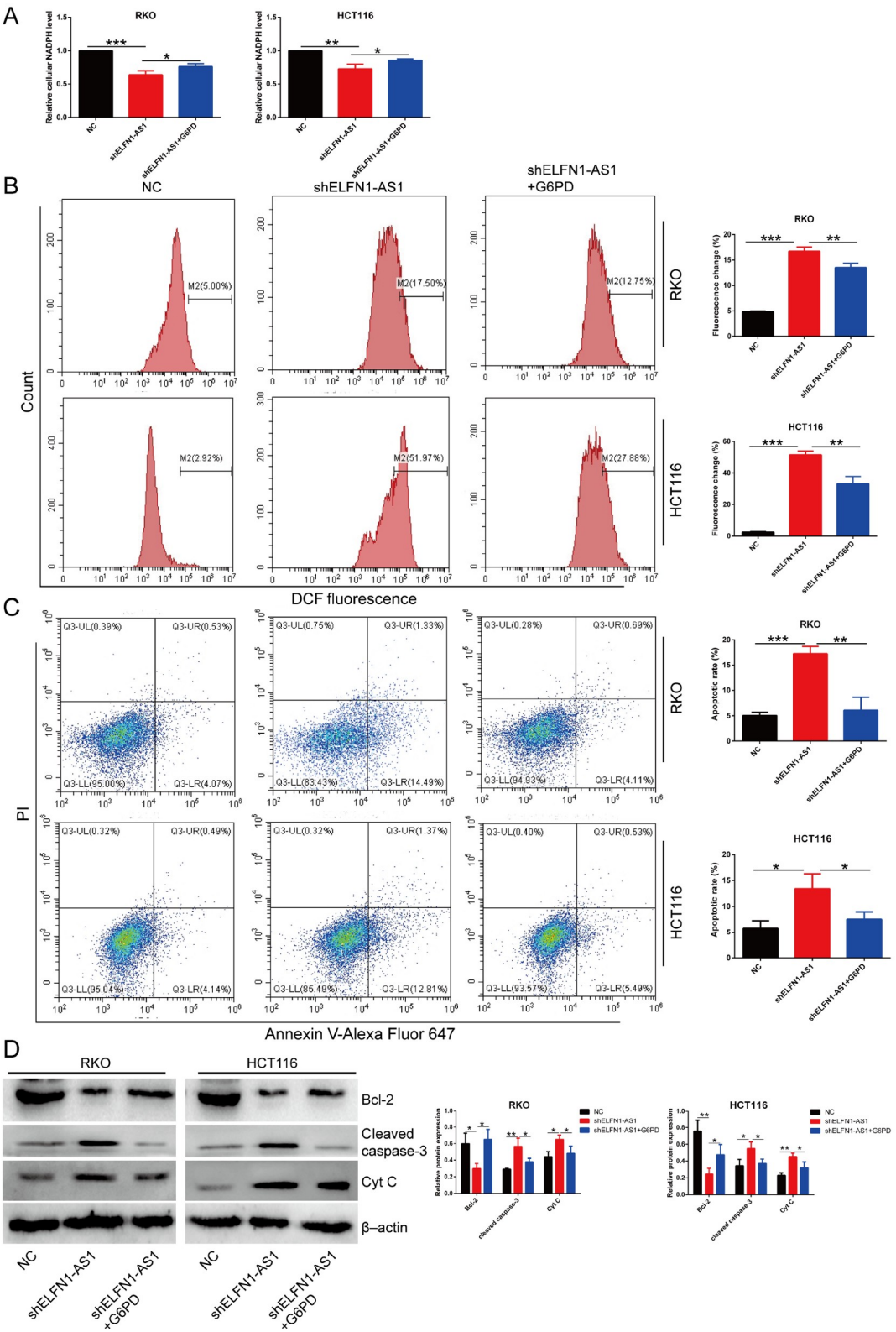

Figure 3. Knockdown of *ELFN1-AS1* significantly promotes ROS accumulation and apoptosis in CRC cells (A) NADPH production in CRC cells transfected with the NC construct, shELFN1-AS1 or shELFN1-AS1 + G6PD. (B) Flow cytometry was used to assess ROS accumulation in CRC cells transfected with the NC construct, shELFN1-AS1 or shELFN1-AS1 + G6PD. The histogram shows the fluorescence changes in CRC cells. (C) Flow cytometry detection of apoptosis in different groups. The histogram shows the apoptotic rate of CRC cells. (D) Knockdown of *ELFN1-AS1* in CRC cells inhibited the expression of *Bcl-2* and promoted the expressions of *cleaved caspase-3* and *Cyt-C*; however, overexpression of *G6PD* blocked these effects. Data are shown as the mean ± SD. $^{*}P < 0.05$, $^{**}P < 0.01$, $^{***}P < 0.001$.

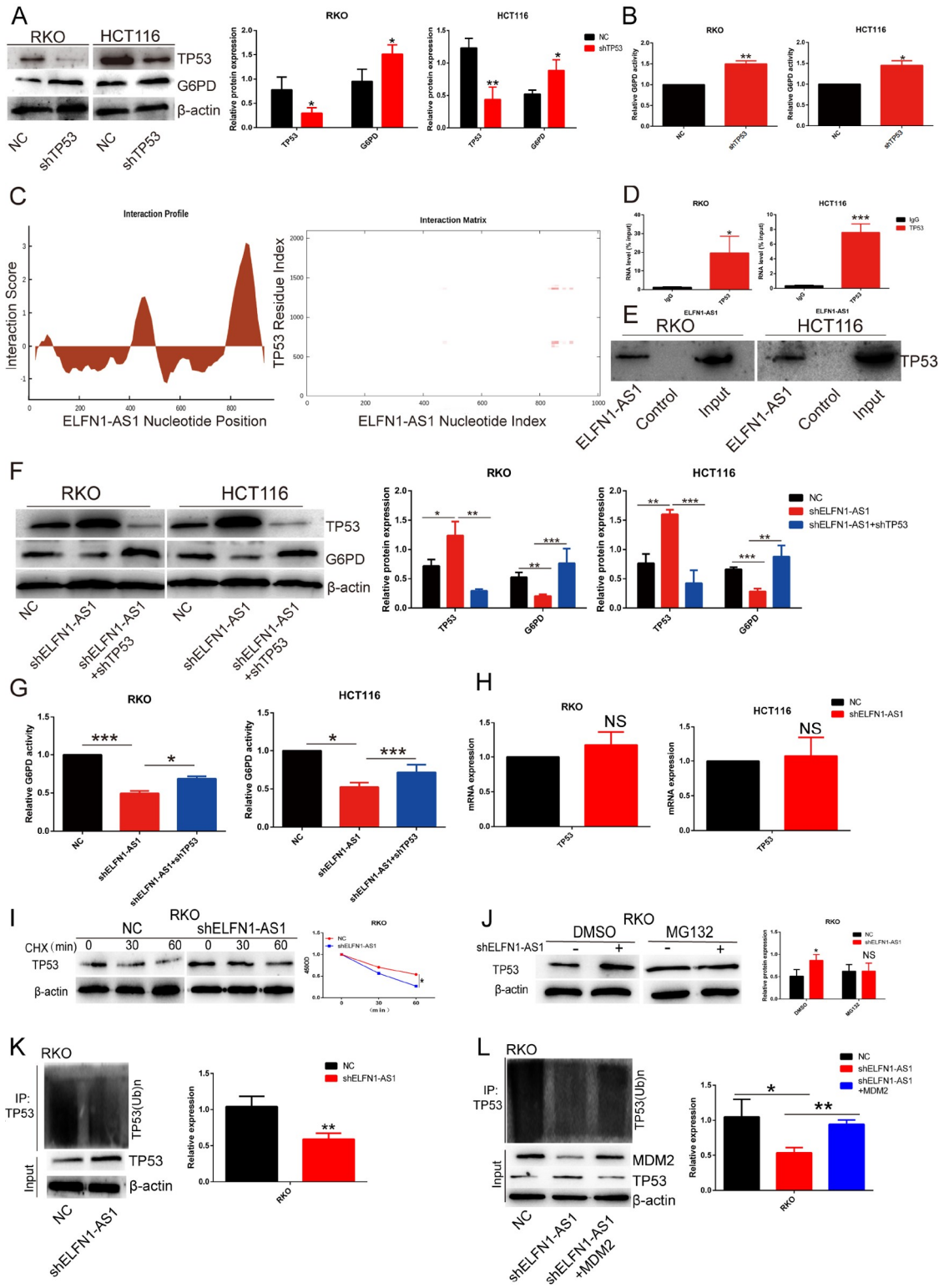

Figure 4. *ELFN1-AS1* regulates *G6PD* expression and activity by *TP53* degradation (A,B) *G6PD* protein expression and activity in *TP53*-knockdown CRC cells. (C) CatRAPID was used to predict the interaction profile and matrix between *TP53* and *ELFN1-AS1*. (D) RIP was used to detect *TP53* binding to *ELFN1-AS1* in RKO and HCT116 cells. *ELFN1-AS1* levels were detected by qPCR and normalized to input levels. (E) Proteins were extracted from CRC cells for biotin-labelled RNA pull-down assays. *ELFN1-AS1*-related proteins were detected by western blot analysis using anti-*TP53* antibody. (F,G) Detection of *G6PD* protein expression and activity in different groups. (H) *TP53* mRNA expression. (I)Treatment of RKO and HCT116 with cycloheximide (CHX) increased the stability of *TP53* protein in the shELFN1-AS1 group. (J) The proteasome inhibitor MG132 eliminate the regulatory effect of *ELFN1-AS1* knockdown on *TP53* expression. (K,L) Knockdown of *ELFN1-AS1* reduced the ubiquitination of *TP53*, while overexpression of MDM2 attenuated this inhibition. Data are shown as the mean ± SD. $*P < 0.05$, $**P < 0.01$, $***P < 0.001$.

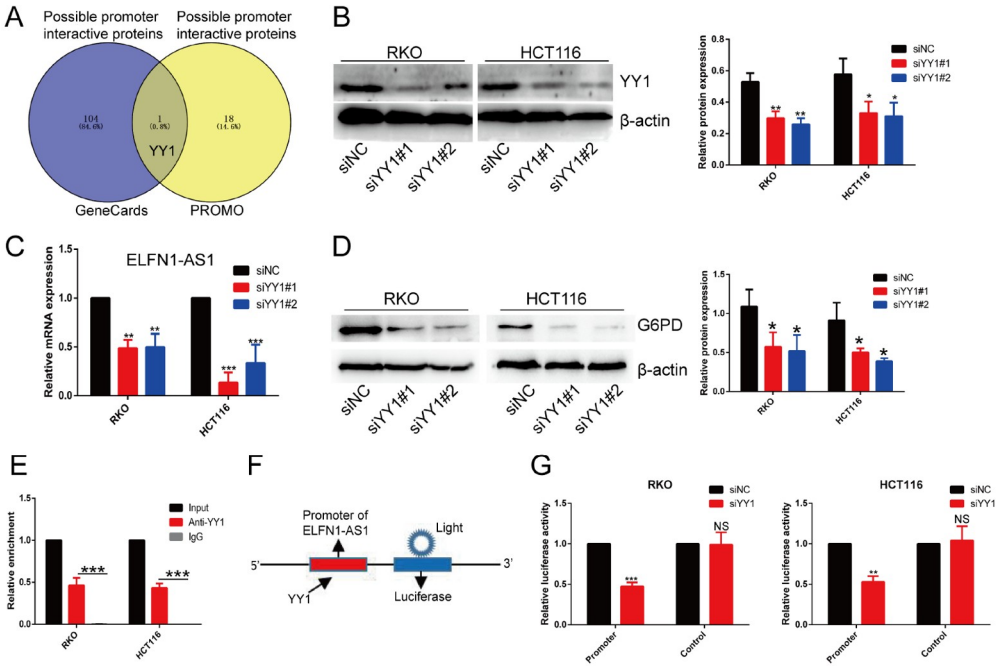

Figure 5. *YY1* promotes *ELFN1-AS1* transcription in CRC cells (A) The PROMO and GeneCards databases were used to predict the transcription factors that bind to the promoter of *ELFN1-AS1*, and the results are shown in a Venn diagram. (B) Detection of the knockdown efficiency of *YY1* by western blot analysis. (C,D) In RKO and HCT116 cells, knockdown of *YY1* inhibited *ELFN1-AS1* and *G6PD* expression. (E) PCR results of ChIP experiment. (F,G) The *ELFN1-AS1* promoter was inserted into the 5′ end of the luciferase gene and the fluorescence was detected. Knockdown of *YY1* inhibited the luciferase activity of constructs containing the *ELFN1-AS1* promoter, but there was no significant change in the activity of the control reported. Data are shown as the mean ± SD. $*P<0.05$, $**P<0.01$, $***P<0.001$.

potential molecular mechanisms leading to the development of CRC are still unclear [26]. *ELFN1-AS1* is a novel primate lncRNA, and it is the antisense RNA of *ELFN1* and is expressed mainly in human tumours [27]. In this study, we revealed that *ELFN1-AS1* expression was increased in both CRC tissues and cells, and these results were consistent with findings in ovarian, oesophageal, colorectal, and retinoblastoma cancers [20,22,23,28,29]. Metabolic alteration is an important hallmark of tumour cells that confers a growth advantage. We revealed that knockdown of *ELFN1-AS1* inhibited glucose consumption and lactate production in tumour cells, thereby linking *ELFN1-AS1* with metabolic reprogramming in tumour cells.

G6PD, the first rate-limiting enzyme of the PPP, plays a key role in tumour development. Overexpression of *G6PD* enhances cancer cell survival via the production of NADPH, which can be used for reductive biosynthesis and antioxidant defence [30]. Studies have shown that *G6PD* plays an important role in tumor cell progression and is significantly upregulated in most tumor tissues. It may be related to the fact that *G6PD* provides NADPH to tumours through the activation of *c-Src*, thus providing important raw materials for the rapid proliferation of tumour cells [31]. In our experiment, we found that *ELFN1-AS1* promoted glucose consumption and lactate production and demonstrated that *ELFN1-AS1* enhanced the PPP via *G6PD* in CRC cells. These results suggested that *ELFN1-AS1* activated the PPP pathway through *G6PD*.

Elevated ROS levels are thought to be carcinogenic, causing damage to DNA, proteins and lipids and promoting genetic instability and tumorigenesis [32]. The PPP, a branch of glycolysis catalysed by hexokinase, uses glucose-6-phosphate as the main substrate and is the main pathway for the synthesis of ribonucleotides and NADPH [6].NADPH plays a critical role in controlling high levels of ROS in rapidly proliferating cancer cells [33]. Excessive production of ROS can cause cytotoxicity and result in DNA damage and apoptosis [34]. In this study, we found that downregulation of *ELFN1-AS1* expression promoted ROS accumulation and apoptosis in CRC cells by inhibiting *G6PD* activity and that these results were caused by reduced production of NADPH. By using western blot analysis, we found that knockdown of *ELFN1-AS1* inhibited *Bcl-2* expression and promoted the expressions of cleaved caspase-3 and *Cyt-C*. Our study suggests that *ELFN1-AS1* promotes NADPH production by enhancing *G6PD* activity, thereby reducing ROS accumulation and apoptosis in tumours.

TP53 is a key suppressor of tumorigenesis [35]. It has been verified that *MDM2* is an E3 ubiquitin ligase involved in ubiquitin-dependent proteasomal degradation of target proteins, and the protein stability and function of *TP53* are regulated by *MDM2*. *MDM2* directly inhibits *TP53* transcriptional activity and targets *TP53* degradation by binding to its transcriptional activation domain [36]. In addition, *TP53* can directly interact with *G6PD* and inhibit its activity, thereby inhibiting the PPP [37]. Our findings suggested that *TP53*, regulated by *ELFN1-AS1*, can inhibit the expression of *G6PD* protein. To further explore the modification of *ELFN1-AS1* and *TP53* to regulate *G6PD*, we investigated the specific mode of action between *ELFN1-AS1* and *TP53*, and found that knockdown of *ELFN1-AS1* enhanced the protein stability of *TP53* by reducing its ubiquitination. Our findings demonstrated that knockdown of *ELFN-AS1* resulted in an increase of *TP53* protein, which is dependent on *MDM2*-mediated ubiquitination.

YY1 is a versatile transcription factor that activates or represses the transcription of target genes depending on the environment and

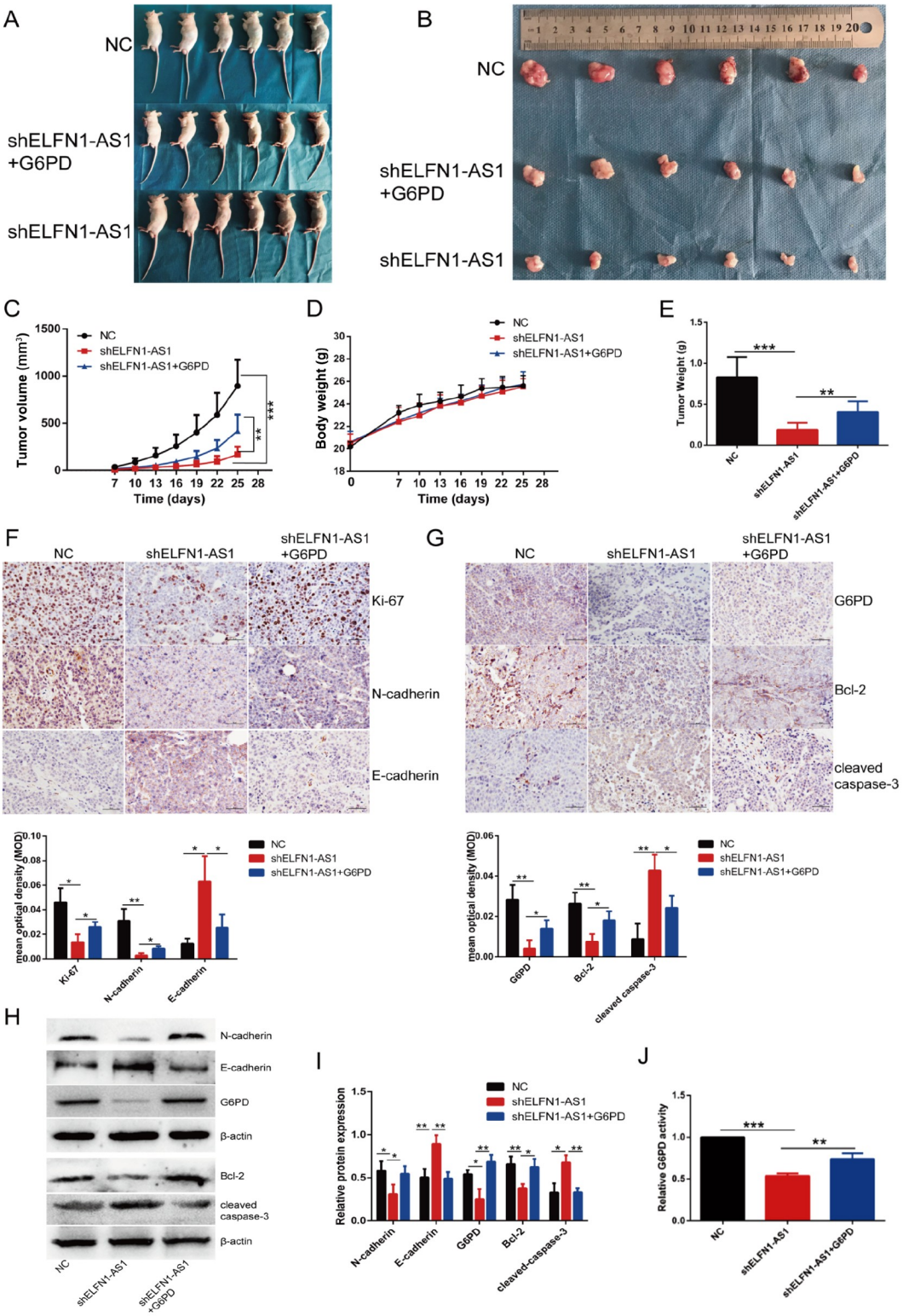

Figure 6. Downregulation of *ELFN1-AS1* decreases the tumorigenicity of CRC cells *in vivo* (A,B) Images of tumours from nude mice in the NC, shELFN1-AS1 and shELFN1-AS1 + G6PD groups are shown. (C) The tumour volumes of the different groups were measured at the specified time points. (D) The body weights of nude mice were not significantly different among the three groups. (E) Tumour weight in the different groups. (F,G) IHC images of *Ki-67*, *N-cadherin*, *G6PD*, *Bcl-2*, *E-cadherin* and *cleaved caspase-3* in the NC, shELFN1-AS1 and shELFN1-AS1 + G6PD groups are shown (scale bar = 50 μm). The histogram shows the MOD of the IHC images. (H,I) Western blot analysis results showed that compared with those in the NC group, *Ki-67*, *N-cadherin*, *G6PD* and *Bcl-2* expressions in tumour tissues were downregulated in the shELFN1-AS1 group, while *E-cadherin* and *cleaved caspase-3* expressions were upregulated. Further studies revealed that overexpression of *G6PD* hindered this effect. (J) *G6PD* activity among the three groups. Data are shown as the mean ± SD. $*P < 0.05$, $**P < 0.01$, $***P < 0.001$.

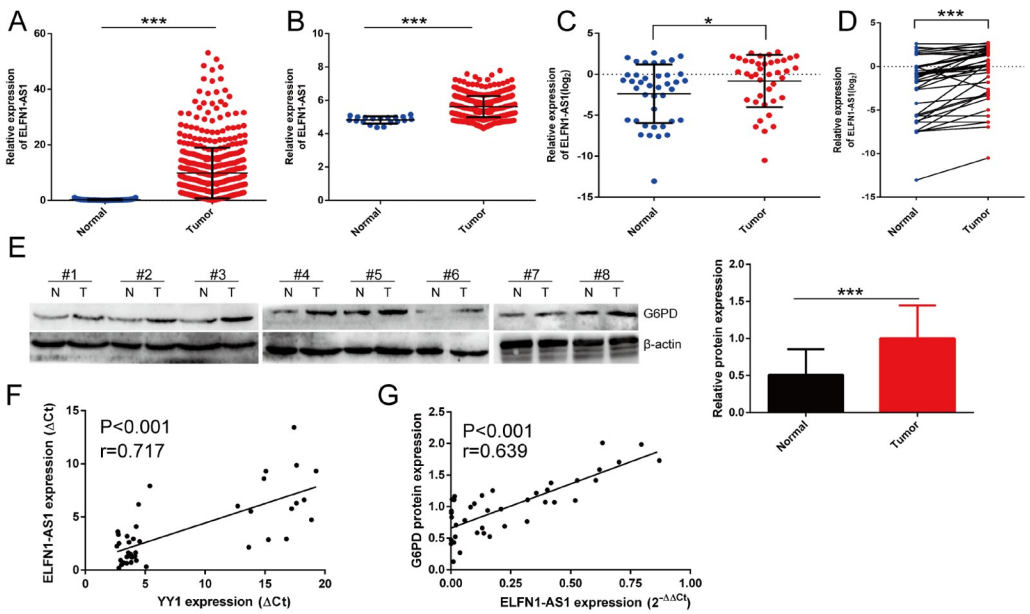

Figure 7. Correlations of *ELFN1-AS1*/*G6PD* co-expression with clinicopathological characteristics (A) TCGA database analysis revealed that *ELFN1-AS1* is upregulated in CRC. (B) The GSE39582 database showed that *ELFN1-AS1* is upregulated in CRC. (C, D) The expression of *ELFN1-AS1* in CRC tissues and matched normal tissues was measured by qRT-PCR. (E) Western blot analysis was performed to detect *G6PD* expression in CRC tissues and matched normal tissues. (F) Correlation analysis of *ELFN1-AS1* and *YY1* expression in CRC tissues. (G) Correlation analysis of *ELFN1-AS1* and *G6PD* protein expression in CRC. $^{*}P<0.05$, $^{***}P<0.001$.

the recruitment of particular cofactors [38]. Although Wu *et al.* [3] found that *YY1*-binding *G6PD* still regulates the PPP in *TP53* mutants, they did not investigate whether *YY1* can regulate the PPP through *TP53*. Our study revealed that *YY1* binds to the promoter of *ELFN1-AS1* to promote *ELFN1-AS1* transcription, after which *ELFN1-AS1* binds to *TP53* to promote *G6PD* activity. In summary, the *YY1*/*ELFN1-AS1*/*TP53*/*G6PD* axis regulates tumour growth in CRC.

Nevertheless, there are still several limitations here. First, this study was performed only in RKO and HCT116 cells, not in other CRC cell lines, and the number of clinical samples collected for the experiment was limited. Second, our study mainly focused on the *YY1*/*ELFN1*/*TP53*/*G6PD* axis, but the effectiveness of targeting CRC via this axis needs to be further explored. In addition further studies are needed to assess whether the enhancement of the PPP in normal cells with high proliferative capacity or in an inflammatory environment is also regulated by *ELFN1-AS1*.

In summary, our study suggested that *ELFN1-AS1* promotes cell proliferation, migration and invasion and inhibits cellular ROS accumulation and apoptosis by increasing *G6PD* activity *in vivo* and *in vitro*. In addition, we showed that *ELFN1-AS1* promoted glucose consumption, lactate and NADPH production, and *ELFN1-AS1* enhanced *G6PD* expression and activated the PPP by *TP53* degradation. Furthermore, the transcription factor *YY1* binds to the *ELFN1-AS1* promoter to promote the transcription of *ELFN1-AS1*. We for the first time identified the *YY1*/*ELFN1-AS1*/*TP53*/*G6PD* axis in CRC cells. Our findings facilitate the elucidation of the regulatory network of *ELFN1-AS1* in CRC, providing valuable biomarkers and possible therapeutic targets for the clinical treatment of CRC.

Supplementary Data

Supplementary data is available at *Acta Biochimica et Biphysica Sinica* online.

Funding

This work was supported by the grants from the National Natural Science Foundation of China (No. 82060800), the Doctoral students Training Research Fund of Lanzhou University Second Hospital (No. YJS-BD-32), and the Science and technology projects in Chengguan District of Lanzhou City (No. 2014-4-4).

Conflict of Interest

The authors declare that they have no conflict of interest.

References

1. Pavlova NN, Thompson CB. The emerging hallmarks of cancer metabolism. *Cell Metab* 2016, 23: 27–47
2. Warburg O. On the origin of cancer cells. *Science* 1956, 123: 309–314
3. Wu S, Wang H, Li Y, Xie Y, Huang C, Zhao H, Miyagishi M, *et al.* Transcription factor YY1 promotes cell proliferation by directly activating the pentose phosphate pathway. *Cancer Res* 2018, 78: 4549–4562
4. Sun L, Suo C, Li S, Zhang H, Gao P. Metabolic reprogramming for cancer cells and their microenvironment: beyond the Warburg effect. *Biochim Biophys Acta Rev Cancer* 2018, 1870: 51–66
5. Kroemer G, Pouyssegur J. Tumor cell metabolism: cancer's achilles' heel. *Cancer Cell* 2008, 13: 472–482
6. Patra KC, Hay N. The pentose phosphate pathway and cancer. *Trends Biochem Sci* 2014, 39: 347–354
7. Chen Q, Wei C, Wang Z, Sun M. Long non-coding RNAs in anti-cancer drug resistance. *Oncotarget* 2017, 8: 1925–1936
8. Iyer MK, Niknafs YS, Malik R, Singhal U, Sahu A, Hosono Y, Barrette TR, *et al.* The landscape of long noncoding RNAs in the human transcriptome. *Nat Genet* 2015, 47: 199–208
9. Xu S, Wang Q, Kang Y, Liu J, Yin Y, Liu L, Wu H, *et al.* Long noncoding RNAs control the modulation of immune checkpoint molecules in cancer. *Cancer Immunol Res* 2020, 8: 937–951
10. da Rocha ST, Boeva V, Escamilla-Del-Arenal M, Ancelin K, Granier C,

Matias NR, Sanulli S, *et al.* Jarid2 is implicated in the initial Xist-induced targeting of PRC2 to the inactive X chromosome. *Mol Cell* 2014, 53: 301–316

11. Hacisuleyman E, Goff LA, Trapnell C, Williams A, Henao-Mejia J, Sun L, McClanahan P, *et al.* Topological organization of multichromosomal regions by the long intergenic noncoding RNA Firre. *Nat Struct Mol Biol* 2014, 21: 198–206
12. Kurian L, Aguirre A, Sancho-Martinez I, Benner C, Hishida T, Nguyen TB, Reddy P, *et al.* Identification of novel long noncoding RNAs underlying vertebrate cardiovascular development. *Circulation* 2015, 131: 1278–1290
13. Li M, Gou H, Tripathi BK, Huang J, Jiang S, Dubois W, Waybright T, *et al.* An apela RNA-containing negative feedback loop regulates p53-mediated apoptosis in embryonic stem cells. *Cell Stem Cell* 2015, 16: 669–683
14. Venkatraman A, He XC, Thorvaldsen JL, Sugimura R, Perry JM, Tao F, Zhao M, *et al.* Maternal imprinting at the H19–Igf2 locus maintains adult haematopoietic stem cell quiescence. *Nature* 2013, 500: 345–349
15. Zhang J, Zhang P, Wang L, Piao H, Ma L. Long non-coding RNA HOTAIR in carcinogenesis and metastasis. *Acta Biochim Biophys Sin* 2014, 46: 1–5
16. Cai R, Sun Y, Qimuge N, Wang G, Wang Y, Chu G, Yu T, *et al.* Adiponectin AS lncRNA inhibits adipogenesis by transferring from nucleus to cytoplasm and attenuating Adiponectin mRNA translation. *Biochim Biophys Acta Mol Cell Biol Lipids* 2018, 1863: 420–432
17. Chu C, Zhang QC, da Rocha ST, Flynn RA, Bharadwaj M, Calabrese JM, Magnuson T, *et al.* Systematic discovery of Xist RNA binding proteins. *Cell* 2015, 161: 404–416
18. Tay Y, Rinn J, Pandolfi PP. The multilayered complexity of ceRNA crosstalk and competition. *Nature* 2014, 505: 344–352
19. Baranova AV, Lobashev AV, Ivanov DV, Krukovskaya LL, Yankovsky NK, Kozlov AP. In silico screening for tumour-specific expressed sequences in human genome. *FEBS Lett* 2001, 508: 143–148
20. Du Y, Hou Y, Shi Y, Liu J, Li T. Long non-coding RNA ELFN1-AS1 Promoted colon cancer cell growth and migration via the miR-191-5p/special AT-rich sequence-binding protein 1 axis. *Front Oncol* 2020, 10: 588360
21. Zhang C, Lian H, Xie L, Yin N, Cui Y. LncRNA ELFN1-AS1 promotes esophageal cancer progression by up-regulating GFPT1 via sponging miR-183-3p. *Biol Chem* 2020, 401: 1053–1061
22. Jie Y, Ye L, Chen H, Yu X, Cai L, He W, Fu Y. ELFN1-AS1 accelerates cell proliferation, invasion and migration via regulating miR-497-3p/CLDN4 axis in ovarian cancer. *Bioengineered* 2020, 11: 872–882
23. Lei R, Feng L, Hong D. ELFN1-AS1 accelerates the proliferation and migration of colorectal cancer via regulation of miR-4644/TRIM44 axis. *Cancer Biomark* 2020, 27: 433–443
24. Wu F, Wei H, Liu G, Zhang Y. Bioinformatics profiling of five immune-related lncRNAs for a prognostic model of hepatocellular carcinoma. *Front Oncol* 2021, 11: 667904
25. Jiang X, Li C, Lin B, Hong H, Jiang L, Zhu S, Wang X, *et al.* cIAP2 promotes gallbladder cancer invasion and lymphangiogenesis by activating the NF-κB pathway. *Cancer Sci* 2017, 108: 1144–1156
26. Huang JZ, Chen M, Chen D, Gao XC, Zhu S, Huang H, Hu M, *et al.* A peptide encoded by a putative lncRNA HOXB-AS3 suppresses colon cancer growth. *Mol Cell* 2017, 68: 171–184.e6
27. Polev DE, Karnaukhova IK, Krukovskaya LL, Kozlov AP. *ELFN1-AS1*: a novel primate gene with Possible microRNA function expressed predominantly in human tumors. *Biomed Res Int* 2014, 2014: 1–10
28. Dong L, Ding C, Zheng T, Pu Y, Liu J, Zhang W, Xue F, *et al.* Extracellular vesicles from human umbilical cord mesenchymal stem cells treated with siRNA against ELFN1-AS1 suppress colon adenocarcinoma proliferation and migration. *Am J Transl Res* 2019, 11: 6989–6999
29. Feng W, Zhu R, Ma J, Song H. LncRNA ELFN1-AS1 promotes retinoblastoma growth and invasion via regulating miR-4270/SBK1 axis. *CMAR* 2021, Volume 13: 1067–1073
30. Abu el Maaty MA, Dabiri Y, Almouhanna F, Blagojevic B, Theobald J, Büttner M, Wölfl S. Activation of pro-survival metabolic networks by 1,25 (OH)2D3 does not hamper the sensitivity of breast cancer cells to chemotherapeutics. *Cancer Metab* 2018, 6: 11
31. Ma H, Zhang F, Zhou L, Cao T, Sun D, Wen S, Zhu J, *et al.* c-Src facilitates tumorigenesis by phosphorylating and activating G6PD. *Oncogene* 2021, 40: 2567–2580
32. Moloney JN, Cotter TG. ROS signalling in the biology of cancer. *Semin Cell Dev Biol* 2018, 80: 50–64
33. Tedeschi PM, Lin HX, Gounder M, Kerrigan JE, Abali EE, Scotto K, Bertino JR. Suppression of cytosolic NADPH pool by thionicotinamide increases oxidative stress and synergizes with chemotherapy. *Mol Pharmacol* 2015, 88: 720–727
34. Ju HQ, Lin JF, Tian T, Xie D, Xu RH. NADPH homeostasis in cancer: functions, mechanisms and therapeutic implications. *Sig Transduct Target Ther* 2020, 5: 231
35. Lou J, Hao Y, Lin K, Lyu Y, Chen M, Wang H, Zou D, *et al.* Circular RNA CDR1as disrupts the p53/MDM2 complex to inhibit Gliomagenesis. *Mol Cancer* 2020, 19: 138
36. Xu B, Wei Y, Liu F, Li L, Zhou S, Peng Y, Li B. Long noncoding RNA CERS6-AS1 modulates glucose metabolism and tumor progression in hepatocellular carcinoma by promoting the MDM2/p53 signaling pathway. *Cell Death Discov* 2022, 8: 348
37. Jiang P, Du W, Wang X, Mancuso A, Gao X, Wu M, Yang X. p53 regulates biosynthesis through direct inactivation of glucose-6-phosphate dehydrogenase. *Nat Cell Biol* 2011, 13: 310–316
38. Gordon S, Akopyan G, Garban H, Bonavida B. Transcription factor YY1: structure, function, and therapeutic implications in cancer biology. *Oncogene* 2006, 25: 1125–1142